Journal of Applied Geophysics 159 (2018) 540–552

Contents lists available at ScienceDirect

Journal of Applied Geophysics

journal homepage: www.elsevier.com/locate/jappgeo

Calculation of Building Correction for urban gravity surveys. A case study of Athens metropolis (Greece)

S. Dilalos [a,*], J.D. Alexopoulos [a], A. Tsatsaris [b]

[a] National and Kapodistrian University of Athens, Faculty of Geology and Geoenvironment, Department of Geophysics-Geothermic, Panepistiomioupoli Zografou, Greece
[b] University of West Attica, Faculty of Engineering, Department of Surveying and GeoInformatics Engineering, Athens, Greece

ARTICLE INFO

Article history:
Received 8 April 2017
Received in revised form 11 September 2018
Accepted 28 September 2018
Available online 03 October 2018

Keywords:
Building correction
Gravity method
Building density
Building height map
Urban areas

ABSTRACT

In gravity surveys, many unwanted effects are produced by geological or non-geological sources. These calculable effects have to be removed through the data reduction procedure. Common corrections in gravity measurements are those for the instrument drift, the tide, the Free Air, the Bouguer and the terrain effect. However, when we deal with gravity campaigns carried out in cities, we also have to take into consideration the so-called Building Correction. This concerns the correction of the gravitational effect caused by the existence of buildings and anthropogenic constructions (stadiums, bridges etc.) close to a gravity measurement. This process can become quite demanding sometimes. Because of that, in this paper we discuss a calculation method for the Building Correction of the gravity measurements. Two types of data are crucial in that procedure. The first one is the mean building density and the other one is the volume of the existing buildings, which is related to the spatial distribution and the buildings height. The mean building density has been calculated in this paper, based on percentage contribution of the building materials (concrete, bricks etc.) of the whole building volume. The calculated mean building density was equal to 0.44 g/cm^3. A Building Height Map has been produced, based on the Digital Elevation Model and the Digital Surface Model. Taking into account the building volume and their density, a simulation of the terrain correction procedure has been carried out, for the Building Correction calculation. The calculated Building Correction values range from almost zero (in the suburbs) to 0.25 mGal. A comparison for the Residual Anomaly values (affected by the Building Correction) has also been made. Differences up to 0.19 mGal revealed are considered to be quite significant for the credibility of the final data.

1. Introduction

A gravity research was organized and executed in the Athens basin (Greece), with the aim of investigating its geological structure and revealing possible concealed (blind) faults, which could affect the city in the future by generating disastrous earthquakes. The most recent disastrous earthquake, on 7 September 1999, had its epicenter at a fault that had not generated severe earthquakes until then. After that, a number of geological researches began in the area, but Athens basin is covered with artificial constructions (buildings, stadiums, roads, playgrounds, public services station etc.) in a very large percent. This means that many geophysical methods cannot be applied in the area, such as electromagnetics, magnetics and geoelectrics. However, the land gravity measurements seem like a cost-effective method for structural investigation. However, Athens, as an urban area produces a non-geological additional gravitational effect to the field measurements, due to the anthropogenic constructions (buildings, constructions etc.). For that reason, in this paper we introduce a computational method of removing the buildings gravitational effect.

Athens basin, as a complex neotectonic graben, is covered with post-alpine sediments (Fig. 3). It is elongated in a NE-SW direction, surrounded by Parnitha (*NW*), Penteli (*NE*), Hymettus (*E*), Aigaleo-Poikilo(*W*) Mountains, while at South it is facing to the sea and Saronikos Gulf. Geologically, the surrounding mountains and hills are structured by alpine formations. They are separated tectonically by a large-scale detachment zone (Papanikolaou and collaborators, 2002; Papanikolaou and Papanikolaou, 2007), in two rock types. At the eastern margin, the metamorphic formations of the Attico-Cycladic massif are located, comprising the relatively autochthonous geotectonic unit. At the northern and western margins the unmetamorphic formations appear, known as the Ypopelagoniki unit (Fig. 3).

The metamorphic formations that we come along are mainly marbles, schists and dolomites, dipping towards NW under the unmetamorphic formations (*Ypopelagoniki Unit*), comprised of limestones and alterations of sandstones and shales, with a general trace direction NE-SW(Fig. 3). The hills located in the central and western areas of the basin are constituted by semi-metamorphic rocks and more specifically by an overlying layer of limestones and an underlying mélange

* Corresponding author.
E-mail addresses: sdilalos@geol.uoa.gr (S. Dilalos), jalexopoulos@geol.uoa.gr (J.D. Alexopoulos), atsats@teiath.gr (A. Tsatsaris).

https://doi.org/10.1016/j.jappgeo.2018.09.036
0926-9851/

(sandstones, clays, sandstone marls, tuffs and schists) known as *Athens Schists*. Finally, the *Alepovouni* Unit, observed across the eastern basin and western foothills of Hymettus Mountain, is located tectonically impacted, between the underlying Metamorphic Unit and the overlying Athens Unit. Its upper part consists of compact crystalline limestones while the lowest part is comprised of metamorphic to semi-metamorphic layers of micaceous schists and phyllites.

Gravity measurements have been applied widely the last few years. Their main applications are the structural / basin investigations (Braitenberg et al., 2006; de Castro et al., 2014; Dilalos, 2018; Dilalos and Alexopoulos, 2017; Karner et al., 2005; Madon and Watts, 1998; Onal et al., 2008; Zheng et al., 2006) and the oil-gas or mineral exploration (Chen et al., 2015;Martinez et al., 2013; Wang et al., 2012).

Gravity measurements are affected by many parameters (topography, sea level, elevation etc.) which need to be reduced by the application of the proper corrections. As the first step of the data reduction process, we have to apply the drift and tide corrections. Afterwards, we apply the Free Air Correction, calculating the Simple Bouguer Anomaly. The application of the Terrain Correction follows, in order to calculate the Complete Bouguer Anomaly, which contains both the Regional and the Residual (local) anomalies. In other types of gravity surveys, like micro-gravity, more corrections have to be applied, like the one for the atmospheric pressure (Nozaki and Kanemori, 1996).

Similarly, the present research is considered a typical gravity survey. Although, the urban environment in which it took place, enforces the authors to calculate and apply one additional crucial correction that is required to the field measurements. Buildings that spread perimetrically the gravity stations, establish a certain mass volume above the ground level, where the gravity measurements are collected. This volume is defined by the height and expansion of these buildings. The term “Building Correction” is proposed for the procedure that needs to be done in order to calculate the gravitational effect that is produced by the existence of buildings and anthropogenic constructions (stadiums, malls etc.) close to a gravity station. It refers only to the building mass above the ground, and will be removed from the field measurement.

Several researchers have worked on the building effect and some of them have tried to quantify it. Most of them have based their calculations on Nagy (1966), who calculated the gravitational attraction of a rectangular prism. Radogna etal. (2003) carried out a micro-gravity study for the metro line of Lausanne city, where they calculated the building effects through a software. Detailed work for the correction of building effects is illustrated by Debeglia and Dupont (2002), by modelling the buildings with polygonal prisms. The isolated effects of the walls, the basements and the floors are also presented in this paper. Szeto (2006) calculated the building density equal to 0.58 g/cm^3 ($\pm$ 0.06), considering a box-like building. Panisova et al. (2012; 2014) introduced a microgravity survey in the interior of a church, where photogrammetry has been used to estimate the gravitational effect of the church itself. Finally, Yu (2014) investigated the building effect, adjacent to a new-developed city and a line of buildings. He carried out several gravity profiles parallel to this building line, with increasing distance from them.

2. Data and method

2.1. Data acquisition

A gravity survey was planned with stations placed on a grid, with a view to covering the basin of Athens. The initial grid cell size was set to 1000 m, based on the results of older gravity studies in the area (Papadopoulos and collaborators, 2003; Papadopoulos et al., 2007). Due to the difficulties of an urban geophysical survey, some stations were re-located a few meters. The maximum offset was almost 100 m, trying to avoid the immediate adjacency with large buildings. Great care had been given not only to the primary map planning, but also during the field measurements. At each gravity station, at least two measurements were collected in order to achieve a good repeatability (<0.01mGal). If it was necessary (noisy environment), additional measurements were collected until the desired result. Finally, a repeatability of $\pm$0.007 mGal was accomplished. The gravity stations had to be placed in “open” areas like parks (Fig. 1), fields (Fig. 2), squares, parking areas, home sites etc., trying to keep a distance of at least 75 m from buildings. This distance was selected in an effort to minimize the final effect, based on the results of other studies regarding the building effects (Debeglia and Dupont, 2002; Nowell, 1999; Yu, 2014). Moreover, busy roads had

Fig. 1. Gravity station in a small park, near buildings.

Fig. 2. Gravity station in a basketball field, with tall Buildings around it.

to be avoided, due to the oscillations they produce on the gravimeter, during the measurements. Keeping up with these limitations is quite difficult in a fully developed residential area, like Athens city, minimizing the available locations for a gravity measurement. Not to mention the difficulty of establishing the appropriate gravity bases network, for which we had to take also into consideration the traffic jam of the city roads.

During summer months, two field campaigns were carried out (2013 and 2014), taking advantage of the diminished traffic jam due to the increased absence of the locals' (vacations). A total number of 807 gravity stations were collected (Fig. 3). The gravity meter LaCoste & Romberg G-496 was used for the data acquisition along with a Differential Global Positioning System (dGPS), in order to calculate the necessary coordinates of each gravity station. The system was compiled by two different, dual-frequency*TopCon HiperPro*GPS antennas and the *static* technique was chosen. The processing results of the dGPS measurements revealed average horizontal deviation of $\pm$1.4 cm and vertical one of $\pm$2.2 cm, which are considered accurate enough.

2.2. Common data reduction procedure

The data reduction procedure will be discussed thoroughly in the next paragraph, with the only exception of the Building correction. First, from the base re-measurements, taking place every 2–3 h, we proceeded with the drift correction of the instrument. Then, the tidal effects are removed with the *Oasis Montaj* software, based on the measurement time of each station. The next step includes the latitude (*WGS84 formula*) and free-air correction, where the calculated coordinates of each gravity station are taken into account. The assumed constant density for the Bouguer correction was set up to 2.67 g/cm^3, generally used by several other researchers in the broader area (Casten and Snopek, 2006; Makris et al., 2013; Papadopoulos et al., 2007). At this point, the Simple Bouguer Anomaly has been calculated.

In order to calculate the necessary terrain correction, we need an accurate Digital Elevation Model (DEM). The procedure is based on the Hammer zones (Hammer, 1939). In this paper, we used the *Gravity and Terrain Correction* extension of *Oasis Montaj* for the terrain calculation. An inner radius equal to 1.500 m had been set, along with an outer radius distance equal to 21 km. These lengths were established taking into consideration previous studies in the area (Papadopoulos et al., 2007) as well as the instructions of the software (Geosoft, 2010). Normally, with the aim of calculating the Complete Bouguer Anomaly only the Terrain corrections need to be added to the Simple Bouguer Anomaly. However, in this urban geophysical survey, we also have to calculate and add the Building Correction, because of the building effects.

3. Building Correction

3.1. Building coverage and volume

The first problem we have to deal with is to calculate the spatial coverage of the anthropogenic constructions and buildings in the area of interest. Beyond this, it is necessary to obtain data concerning the volume extension of these constructions. In other words, the information of their height extent is also essential, or at least an indirect approach to calculate it: for example based on the number of floors.

There are some methods to retrieve this kind of data. One common example is the town-planning maps that government services hold. This method has been selected and applied to some older microgravity surveys (Radogna et al., 2003). Nevertheless, for such a big area of interest, like Athens basin (almost 720km^2), this seems impractical and endless.

A quick and precise method to calculate the building volume is presented in this paper. Two types of raster data are required. The first one is a detailed Digital Elevation Model (DEM) (Fig. 4). The second package of data provides us with information about the maximum elevation of the covered area, including the anthropogenic constructions. Many people tend to confuse it with a DEM, but the correct term is 'Digital Surface Model' (DSM) (Fig. 5). A DSM can be produced by high accuracy airborne LIDAR data. Nowadays they are used in many cities of the world for several practical applications, in order to calculate the volume of the buildings and produce their 3D reconstruction (Baba et al., 2014; Brédif et al., 2013; Mongus et al., 2014; Yan et al., 2017). LIDAR data

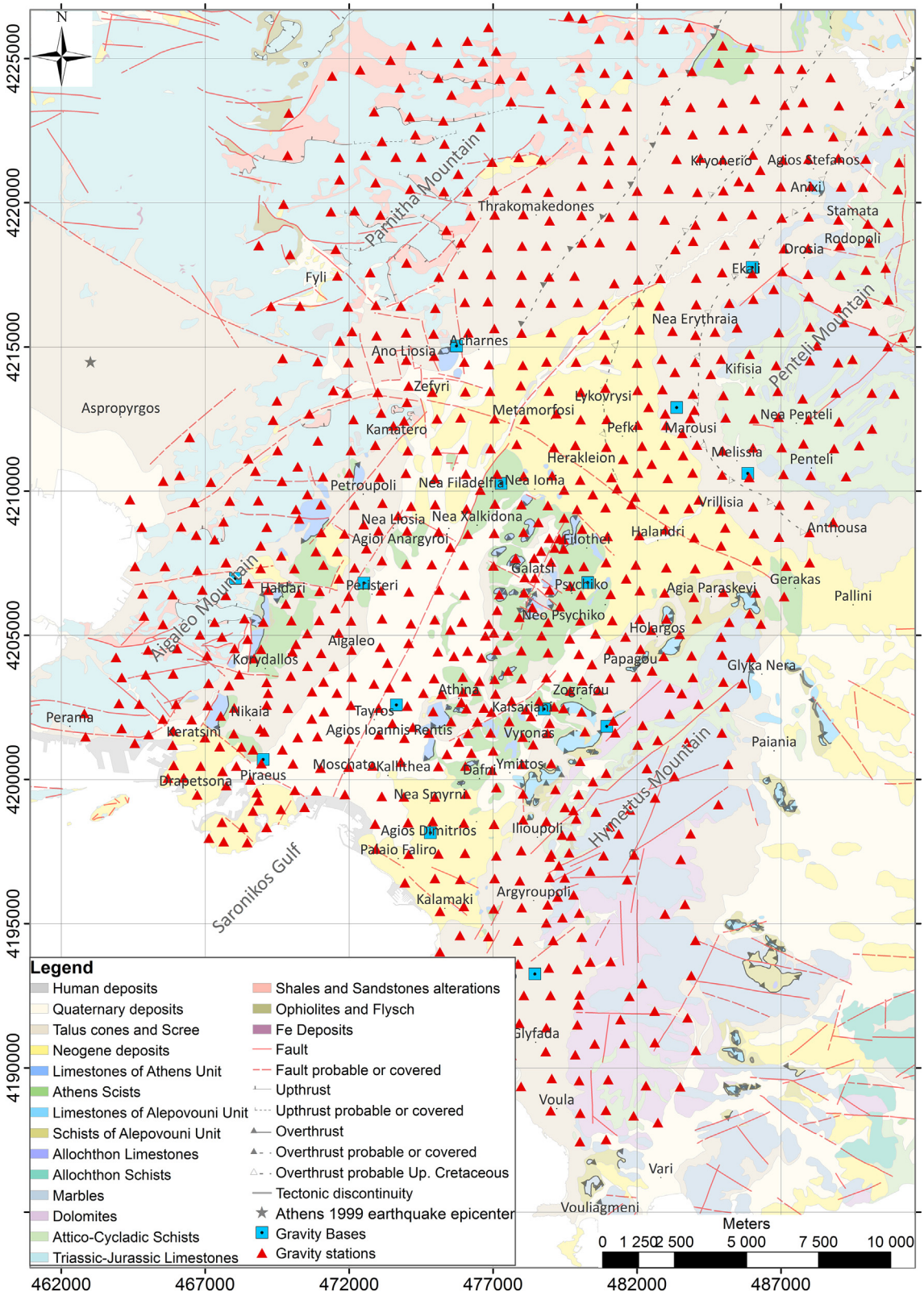

Fig. 3. The locations of the gravity stations and gravity bases.

gives us the maximum elevation points of the investigated area. This means that if a building exists, the elevation of its roof will be measured, as the maximum elevation/surface point. If not, it will measure the terrain elevation (same as in the DEM). Usually, such kinds of data provide a cell size of 0.8–1 m.

Advanced toolboxes of a Geographic Information System and more specifically a raster calculator tool are required in order to proceed. We have to subtract the DEM elevations from the respective DSM elevations (DSM-DEM) (Baba et al., 2014). In that way, a new raster map will be produced, illustrating the heights of all

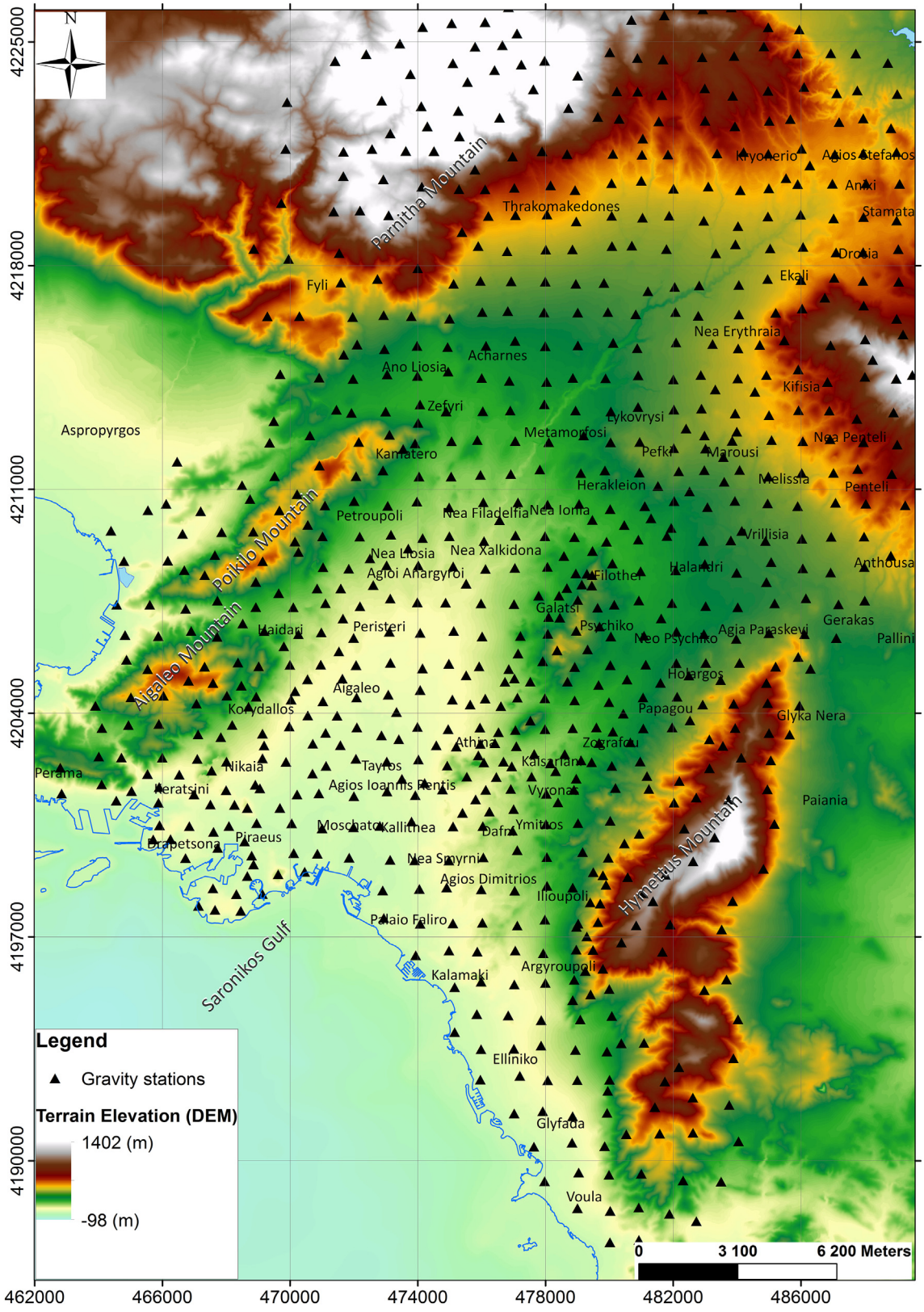

Fig. 4. Digital Elevation Model (DEM).

the buildings and constructions of the investigated area. This is called 'Building Height Map' (Fig. 6). The resulting map will practically illustrate not only the height of the buildings but also their spatial coverage in the area. Although, it might also contain information about the three heights, we consider it negligible, since we are dealing with extremely smaller volumes (coverage and heights at the same time). Great emphasis must be given on the management of the two types of raster maps (DEM and DSM), their cell size and their spatial limits.

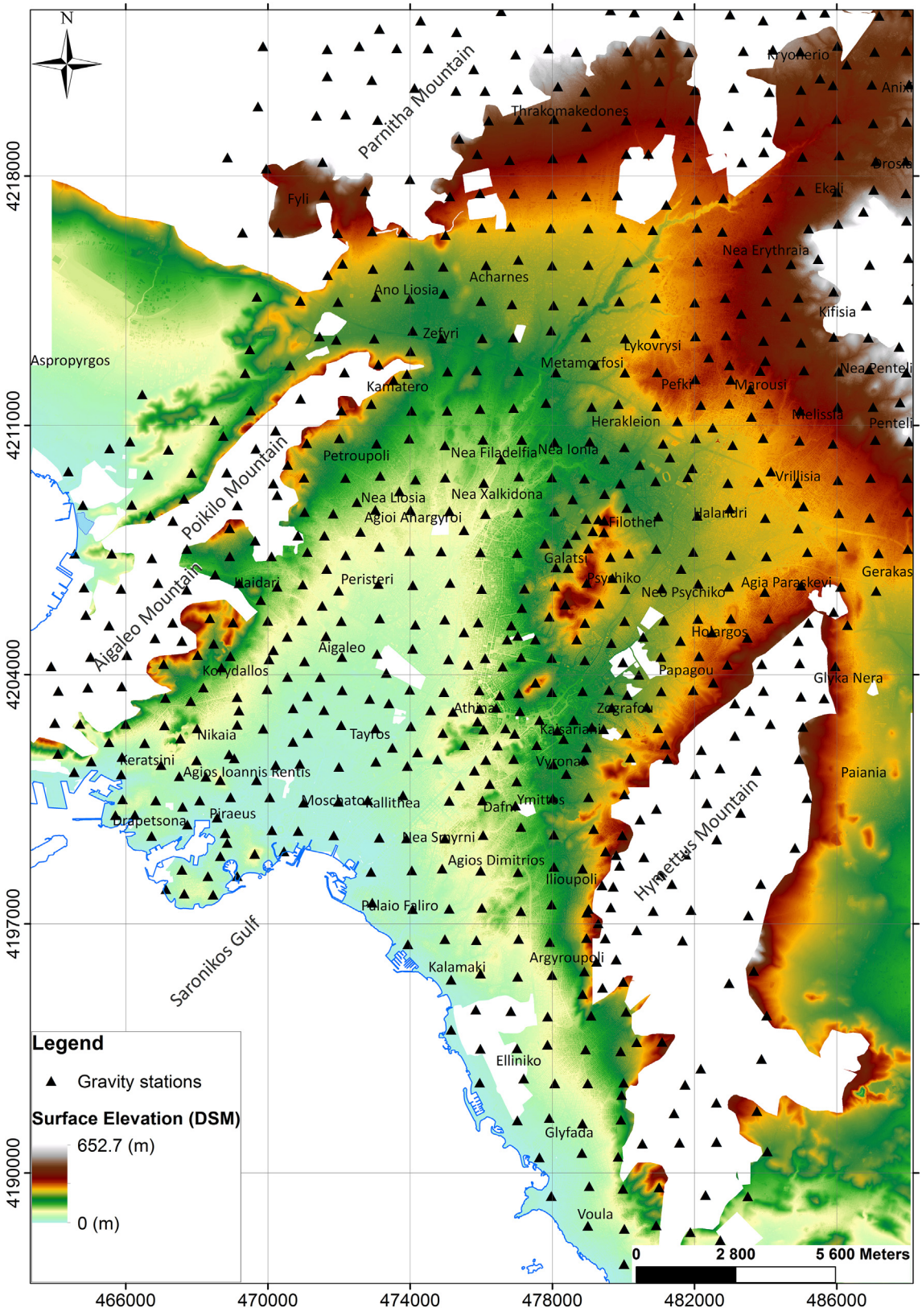

Fig. 5. Digital Surface Model (DSM).

3.2. Building density

In the previous paragraph, a map has been produced demonstrating the spatial distribution and height of all the anthropogenic constructions (Fig. 6). However, the mean density of these buildings is required, in order to calculate the Building Correction of the study area. In a typical city, different types of buildings exist, such as the ones made of stonewalls, wooden walls, concrete, reinforced concrete,

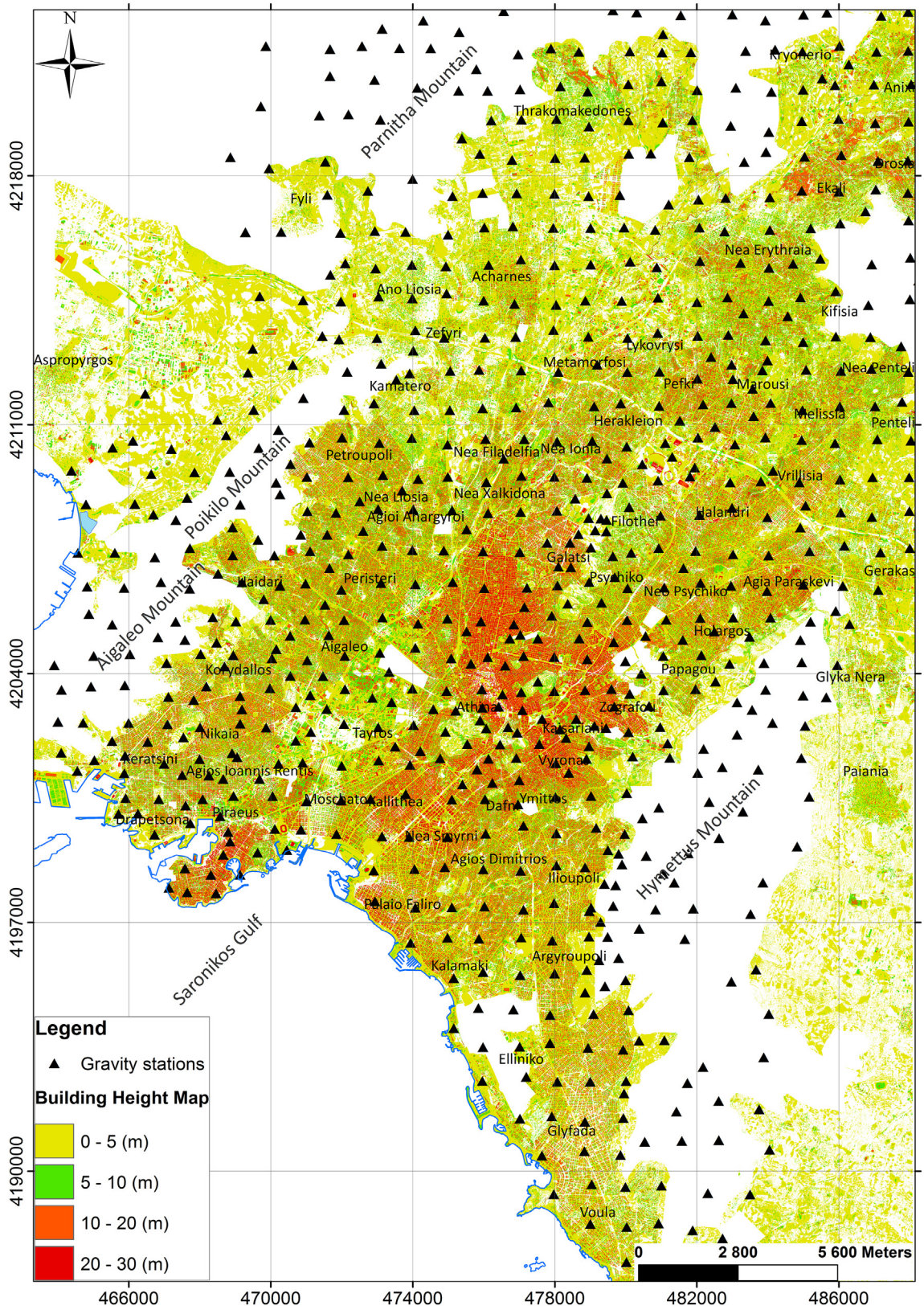

Fig. 6. Building Height Map and the collected gravity stations.

aluminum and glass. In large-scale gravity researches, a mean density of the most common type of building is required. In the city of Athens, the most popular type of building is the one with reinforced concrete and brick walls.

Regarding the structure of this type of buildings and basic aspects of architecture, we have to take into consideration the gravitational attraction of the walls and floor slabs summative. We have to accept some common standards. For example, the thickness of the floor

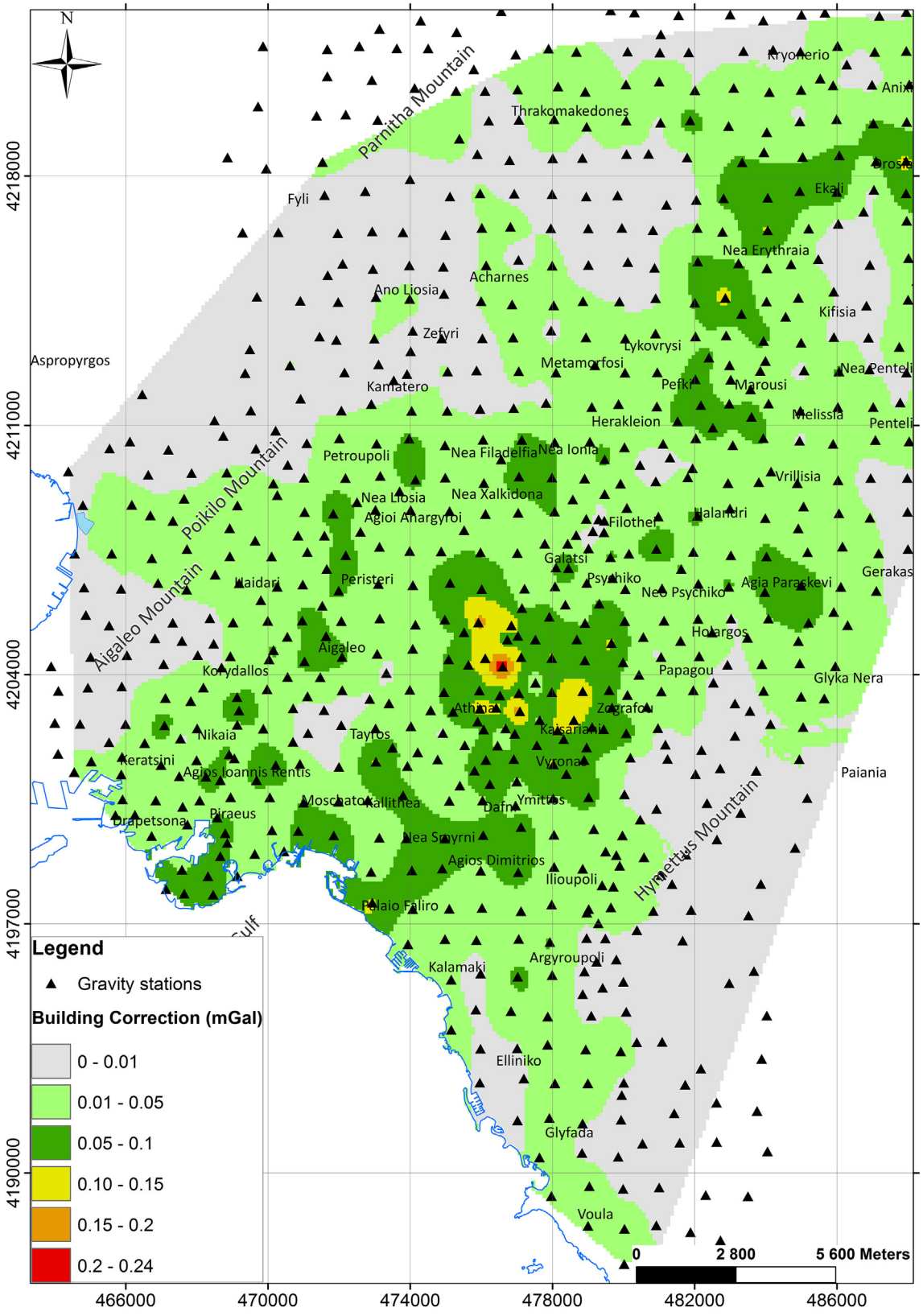

Fig. 7. Building Correction Map along with the collected gravity stations.

concrete slab is usually equal to 0.20 m, the exterior brick wall thickness equal to 0.20 m and the interior ones equal to 0.10 m. Moreover, an average height of an apartment (floor to ceiling) is 2.70 m. After several volume calculations, with a view to estimating the respective participation percent of each building material, it turned out that the concrete contributes 10.5% to the building volume, the brick walls 11% and the air occupies the rest 78.5% of the building. There is also an empirical type of the civil engineers, indicating that the required

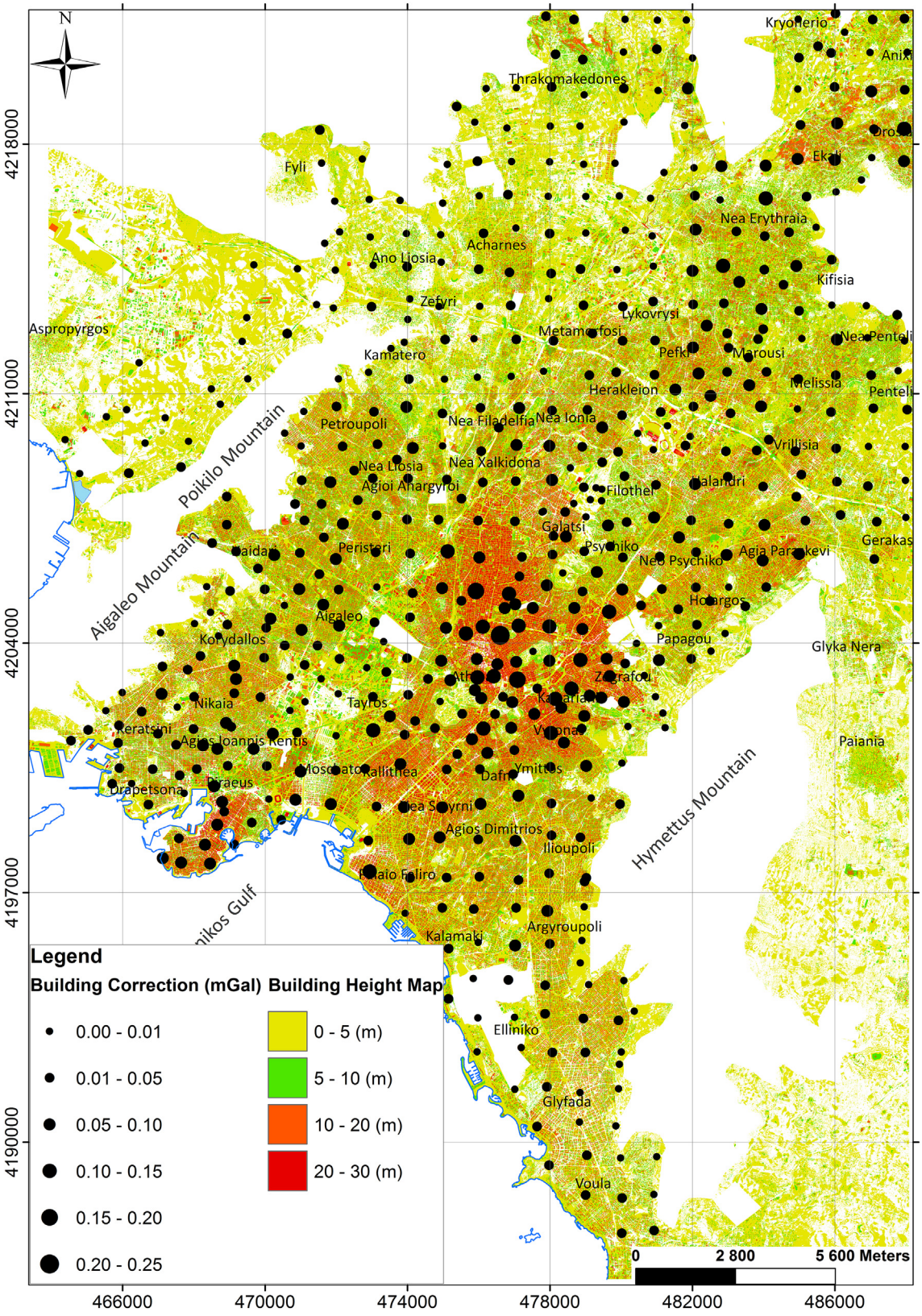

Fig. 8. Building Height Map along with graduated gravity stations based on the values of Building Correction (in mGal).

volume of concrete can be estimated by multiplying the area of the ground plan times 0.3–0.35. This also validates the pre-mentioned calculations.

Several densities concerning the reinforced concrete (Committe A.C.I., 2008; Blake, 2013; Chromčák et al., 2016; Stoulos et al., 2003) have been found. The authors chose a mean reinforced concrete density, equal to 2.4 g/cm^3. Regarding the bricks density (walls), a mean density equal to 1.7 g/cm^3 had been chosen, among several suggested values (Alawadhi, 2008; Ashby and Johnson, 2013; Chromčák et al., 2016; Kuranchie et al., 2016;

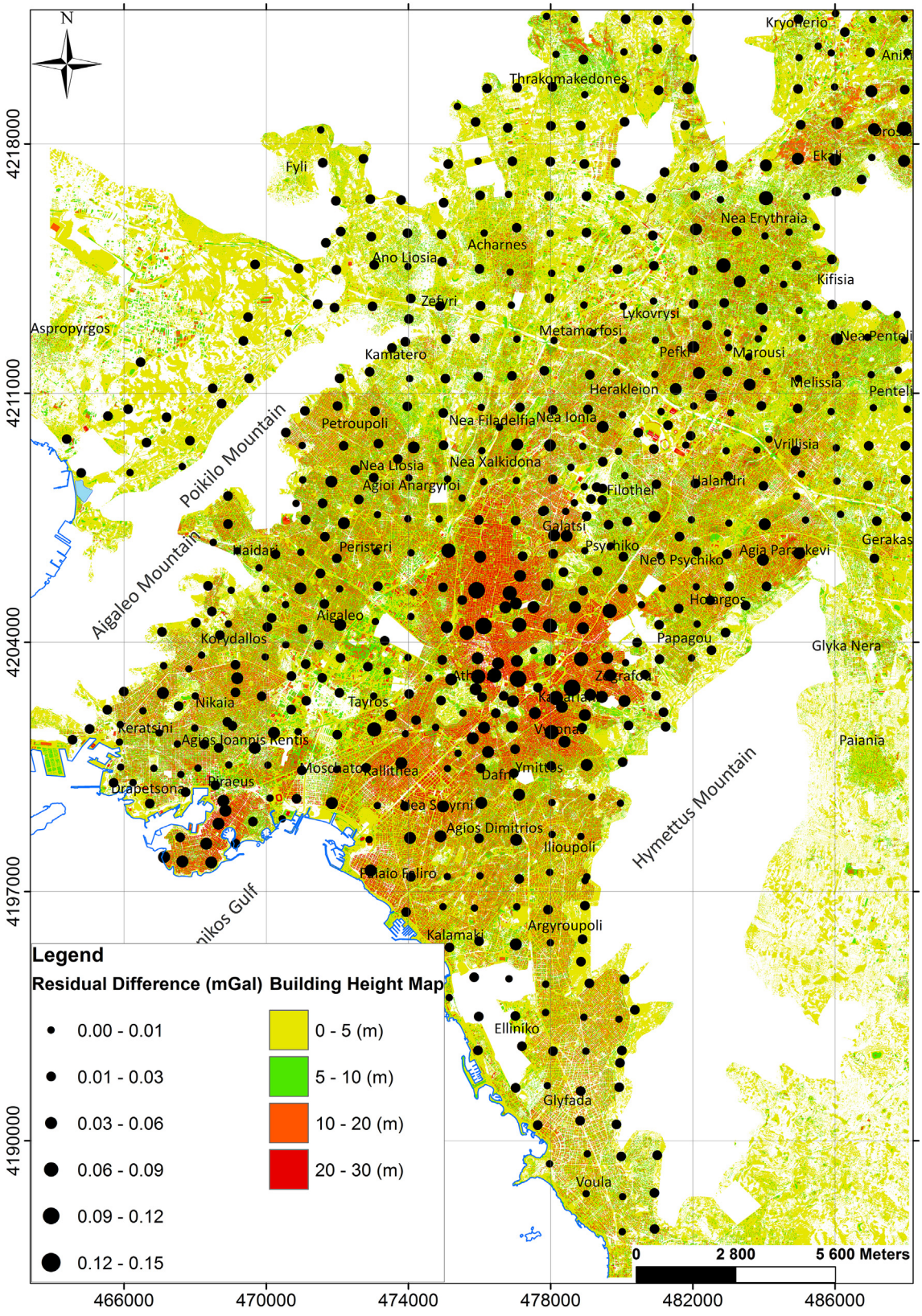

Fig. 9. Building Height Map along with graduated gravity stations based on the final difference of the calculated Residual anomaly.

Stoulos et al., 2003; Jung, 1961). We have to take into consideration the contribution percent of each material, estimated in the previous paragraph, in order to calculate the required building density.

Therefore, we can simply multiply the contribution percent of each material with its characteristic density with the aim of calculating the building's density. The mean density of reinforced concrete building has been calculated equal to 0.44 g/cm^3.Yu (2014) has also calculated a close building density equal to 0.459 g/cm^3 using theoretical building models.

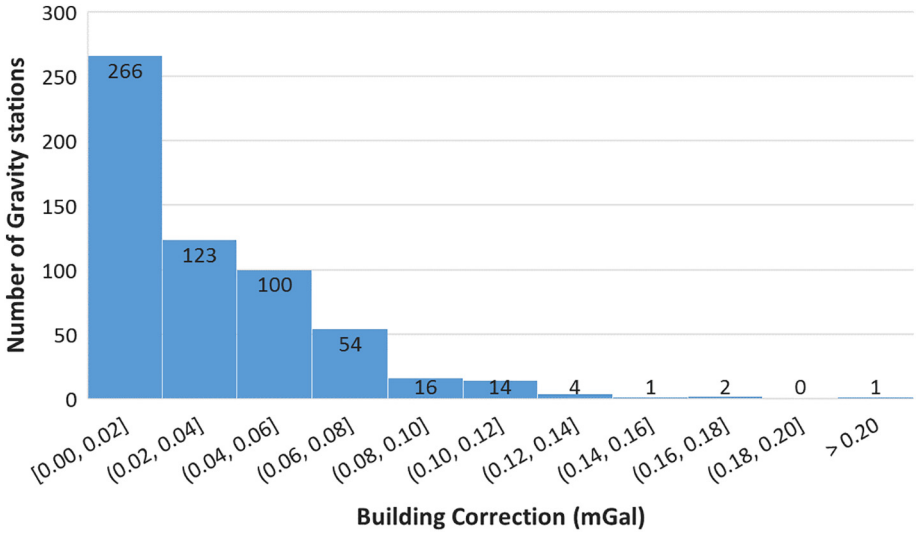

Fig. 10. Building Correction values distribution.

3.3. Calculation and application of building correction

We need two types of data, that is to say the volume of the buildings (Building Height Map –Fig. 6) and their mean density, in order to proceed with the calculation of the Building Correction. The preparation and calculation for both parameters have already been discussed in previous sections of this paper. The procedure is similar to the one for the terrain correction, based on the classic Hammer zones (Hammer, 1939), and carried out through the *Gravity and Terrain Correction* extension of *Oasis Montaj (Geosoft)*. Three parameters have to be changed, in order to obtain the desirable Building Correction.

Firstly, the inner zone radius has been set to 100 m and the outer zone radius to 1000 m, while during the terrain correction calculations, a radius of 1.500 m and another of 21 km respectively have been selected. Beyond these distances, the building effect minimizes rapidly, until it is considered negligible. Secondly, instead of an Elevation input, Building Height (Fig. 6) is required. Thirdly, the reduction density used was the one calculated for the buildings, equal to 0.44 g/cm^3 and not the Bouguer density (2.67 g/cm^3). With only these changes, the procedure of the Building Correction calculations completed (Fig. 7).

The next step is to apply the Building Corrections to the gravity measurements. The reduction procedure is similar to the terrain corrections. After the data reduction of the gravity measurements, the Simple Bouguer Anomaly comes up. Normally, the terrain correction (TC) has to be added, in order to calculate the Complete Bouguer Anomaly (g_{CBA}). However, in the case of an urban geophysical survey, the Building Correction (BC) is necessary to be added to the Simple Bouguer Anomaly (g_{SBA}), like the following equation.

$$g_{CBA} = g_{SBA} + TC + BC$$

After the calculation of the Complete Bouguer Anomaly, the isolation of the Residual Anomaly was carried out. The procedure was based on Fourier analysis and Filtering and the information provided by the corresponding Power Spectrum Analysis (Dilalos, 2018; Dilalos and Alexopoulos, 2017).

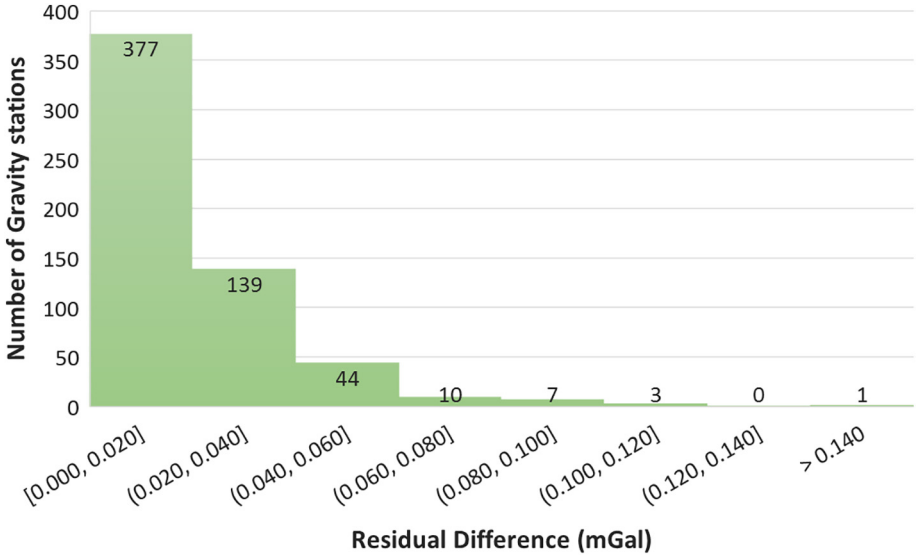

Fig. 11. Histogram distribution of the Residual Anomaly Differences (before and after the Building Correction).

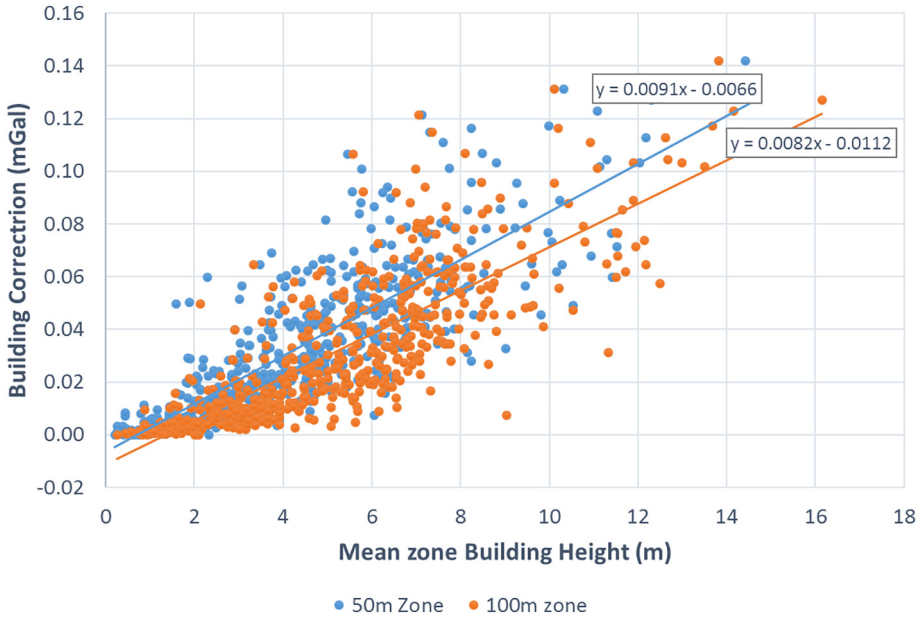

Fig. 12. Correlation of mean Building Height with the respective calculated Building Correction. The blue dots refer to the 50 m radius zone and the red for the 100 m radius zone. (For interpretation of the references to colour in this figure legend, the reader is referred to the web version of this article.)

4. Results

A distribution map of the calculated Building Correction of the study area has been produced (Fig. 7). Moreover, in Fig. 8 the gravity stations and their corresponding calculated Building Correction are illustrated in graduated symbols, based on their value. The Building Height Map has been used as background, providing the capability to correlate the Building Heights with the Building Correction. Therefore, it is obvious that the final correlation is absolutely logic. The highest values of Building Correction correspond to gravity stations that are located in areas with increased building volume, such as the downtown of the city and the area of Piraeus (red areas in Fig. 8). The gravity stations of the mountainous areas are not illustrated in Fig. 8, since there was no need of Building Correction. Residual Anomaly is practically the final processed data that we use for subsurface modelling. Building Correction affects the Complete Bouguer Anomaly and consequently the Residual Anomaly. For that reason, the final difference in Residual Anomaly (before and after the Building Correction) has been investigated and is illustrated in Fig. 9 with graduated symbols. The result is similar, with the most affected gravity stations located in areas with high building volume.

In Fig. 10, we can observe the histogram distribution of the calculated Building Corrections. The calculated values for the entire Athens basin and more precisely for the 582 affected gravity stations (due to the removal of the stations on mountainous areas), begin from zero and reach values of almost 0.25 mGal. Almost half of them (303 of 582 stations) appear with values between zero and 0.02 mGal, which seems negligible. Nevertheless, the other half gravity stations (279 of 582) appear with higher and more significant values of Building Correction.

In Fig. 11, we present the histogram distribution of the final difference values regarding the Residual Anomaly, with and without the addition of the Building Corrections. It is evident that 377 of the 582 stations (after the Building Correction applied on), revealed a final Residual Anomaly difference between zero and 0.02 mGal, which can be considered almost negligible. However, for the other 205 stations, we have significant differences after the application of the calculated Building Corrections, reaching values up to 0.19 mGal.

Finally, an attempt of correlation between the Building Correction and the Height of the surrounding buildings has been made. Two different zones around the stations have been selected (similar to the Hammer zones of the Terrain Correction), one with radius equal to 50 m and one with radius 100 m. The mean Building Height has been calculated for each one of these zones, based on the data of the Building Height Map (Fig. 6). The comparison of the mean Building Height around the gravity stations, with the respective calculated Building Correction, is illustrated in Fig. 12. Of course, we have to take into consideration that the final Building Correction for each gravity station is also influenced by the buildings beyond the zone of 100 m that we have indicated (even in a smaller percent).

5. Conclusions

Building Corrections is an additional but necessary part of gravity data reduction, when the field measurements are carried out in urban areas, with high building volume density. This is originated from the fact that buildings apply additional gravitational attraction to the gravity measurements. It is important to clarify that the proposed correction is not taking into consideration the existence of any basement of the buildings. This is based on the fact that previous studies (Debeglia and Dupont, 2002; Yu, 2014) revealed that the basement effect beyond the 44 m is negligible. In the context of this research, we tried to keep a distance of 75 m from the buildings. Additionally, the DSM data cannot provide information concerning the basement existence.

In this paper, we introduced a computational method for calculating the Building Correction in large-scale gravity surveys, located in residential areas. It is based on a specific data processing procedure, taking advantage of the Digital Elevation Model (DEM) and Digital Surface Model (DSM) of an area, along with a mean building density.

The calculated Building Correction values of the gravity stations vary, from negligible ones in the suburbs (low building volume) to more remarkable ones downtown, up to 0.25 mGal (Figs 8 and 10). Based also on the final impact on the Residual Anomaly values (Figs 9 and 11), with differences up to 0.19 mGal, their calculation is considered quite important.

Urban gravity surveys were considered quite demanding not only for the data acquisition but also for their processing due the buildings

effect. In this paper, we demonstrated a processing method for the Building Correction, with trustworthy results.

Acknowledgments

The fieldwork was supported by the Special Account for Research Grants of the UoA (contract no. 70/4/9254). The authors would like to thank Ms. Achtypi S., Ms. Kaplanidi H., Mr. Papaelias S., Mr. Mavroulis S., Mr. Michelioudakis D.and Ms. Drosopoulou E. for their valuable contribution to the field measurements.

References

Alawadhi, E.M., 2008. Thermal analysis of a building brick containing phase change material. Energy and Buildings 40 (3), 351–357. https://doi.org/10.1016/j.enbuild.2007.03.001.

Ashby, M.F., & Johnson, K., 2013. Materials and Design: The Art and Science of Material Selection in Product Design. Butterworth-Heinemann, 513pp.

Baba, T., Takahashi, N., Kaneda, Y., Inazawa, Y., Kikkojin, M., 2014. Tsunami inundation modeling of the 2011 Tohoku earthquake using three-dimensional building data for Sendai, Miyagi Prefecture, Japan. In: Kontar, Y., Santiago-Fandino, V., Takahashi, T. (Eds.), Tsunami Events and Lessons Learned, Springer Verlag, pp. 89–98.

Blake, L.S. (Ed.), 2013. Civil Engineer's Reference Book. Butterworth-Heinemann (775pp).

Braitenberg, C., Wienecke, S., Wang, Y., 2006. Basement structures from satellite-derived gravity field: South China Sea ridge. Journal of Geophysical Research: Solid Earth 111 (B5). https://doi.org/10.1029/2005JB003938.

Brédif, M., Tournaire, O., Vallet, B., Champion, N., 2013. Extracting polygonal building footprints from digital surface models: a fully-automatic global optimization framework. ISPRS J. Photogramm. Remote Sens. 77, 57–65. https://doi.org/10.1016/j.isprsjprs.2012.11.007.

Casten, U., Snopek, K., 2006. Gravity modelling of the Hellenic subduction zone - a regional study. Tectonophysics 417 (3–4), 183–200. https://doi.org/10.1016/j.tecto.2005.11.002.

Chen, G., Liu, T., Sun, J., Cheng, Q., Sahoo, B., Zhang, Z., Zhang, H., 2015. Gravity method for investigating the geological structures associated with W–Sn polymetallic deposits in the Nanling Range, China. J. Appl. Geophys. 120, 14–25. https://doi.org/10.1016/j.jappgeo.2015.06.001.

Chromčák, J., Grinč, M., Pánisová, J., Vajda, P., Kubová, A., 2016. Validation of sensitivity and reliability of GPR and microgravity detection of underground cavities in complex urban settings: Test case of a cellar. Contributions to Geophysics and Geodesy 46 (1), 13–32. https://doi.org/10.1515/congeo-2016-0002.

Committee, A.C.I., 2008. Building Code Requirements for Structural Concrete (ACI 318–08) and Commentary. American Concrete Institute (1508pp).

de Castro, D.L., Fuck, R.A., Phillips, J.D., Vidotti, R.M., Bezerra, F.H., Dantas, E.L., 2014. Crustal structure beneath the Paleozoic Parnaíba Basin revealed by airborne gravity and magnetic data, Brazil. Tectonophysics 614, 128–145. https://doi.org/10.1016/j.tecto.2013.12.009.

Debeglia, N., Dupont, F., 2002. Some critical factors for engineering and environmental microgravity investigations. J. Appl. Geophys. 50 (4), 435–454. https://doi.org/10.1016/S0926-9851(02)00194-5.

Dilalos, S., 2018. Application of geophysical technique to the investigation of tectonic structures in urban and suburban environments. A case study in Athens basin. Ph. D. Thesis. National and Kapodistrian University of Athens, Athens, Greece 321p.

Dilalos, S., Alexopoulos, J.D., 2017. Indications of correlation between gravity measurements and isoseismal maps. A case study of Athens basin (Greece). J. Appl. Geophys. 140, 62–74. https://doi.org/10.1016/j.jappgeo.2017.03.012.

Geosoft, 2010. Montaj Gravity & Terrain Correction – Gravity Data Processing Extension for Oasis Montaj V.7.1. – Tutorial and User Guide.

Hammer, S., 1939. Terrain corrections for gravimeter stations. Geophysics 4 (3), 184–194. https://doi.org/10.1190/1.1440495.

Jung, K., 1961. Schwerkraftverfahren in Der Angewandten Geophysik. Leipzig, Akademische Verlagsgesellschaft Geest & Portig, 362pp.

Karner, G.D., Studinger, M., Bell, R.E., 2005. Gravity anomalies of sedimentary basins andtheir mechanical implications: Application to the Ross Sea basins, West Antarctica. Earth Planet. Sci. Lett. 235 (3), 577–596. https://doi.org/10.1016/j.epsl.2005.04.016.

Kuranchie, F.A., Shukla, S.K., Habibi, D., 2016. Utilisation of iron ore mine tailings for the production of geopolymer bricks. Int. J. Min. Reclam. Environ. 30 (2), 92–114. https://doi.org/10.1080/17480930.2014.993834.

Madon, M.B., Watts, A.B., 1998. Gravity anomalies, subsidence history and the tectonic evolution of the Malay and Penyu Basins (offshore Peninsular Malaysia). Basin Res. 10 (4), 375–392.

Makris, J., Papoulia, J., Yegorova, T., 2013. A 3-D density model of Greece constrained by gravity and seismic data. Geophys. J. Int. 194 (1), 1–17. https://doi.org/10.1093/gji/ggt059.

Martinez, C., Li, Y., Krahenbuhl, R., Braga, M.A., 2013. 3D inversion of airborne gravity gradiometry data in mineral exploration: a case study in the Quadrilátero Ferrífero, Brazil. Geophysics 78 (1), B1–B11. https://doi.org/10.1190/geo2012-0106.1.

Mongus, D., Lukač, N., Žalik, B., 2014. Ground and building extraction from LiDAR data based on differential morphological profiles and locally fitted surfaces. ISPRS J. Photogramm. Remote Sens. 93, 145–156. https://doi.org/10.1016/j.isprsjprs.2013.12.002.

Nagy, D., 1966. The gravitational attraction of a right rectangular prism. Geophysics 31 (2), 362–371. https://doi.org/10.1190/1.1439779.

Nowell, D.A.G., 1999. Gravity terrain corrections - an overview. J. Appl. Geophys. 42 (2), 117–134. https://doi.org/10.1016/S0926-9851(99)00028-2.

Nozaki, K., Kanemori, T., 1996. Microgravity Survey for Shallow Subsurface Investigations. In: Symposium on the Application of Geophysics to Engineering and Environmental Problems,951-959. Society of Exploration Geophysicists https://doi.org/10.4133/1.2922361.

Onal, K.M., Buyuksarac, A., Aydemir, A., Ates, A., 2008. Investigation of the deep structure of the Sivas Basin (innereast Anatolia, Turkey) with geophysical methods. Tectonophysics 460 (1), 186–197. https://doi.org/10.1016/j.tecto.2008.08.006.

Panisova, J., Pašteka, R., Papco, J., Fraštia, M., 2012. The calculation of building corrections in microgravity surveys using close range photogrammetry. Near Surface Geophysics 10 (5), 391–399. https://doi.org/10.3997/1873-0604.2012034.

Panisova, J., Haličková, J., Brunčák, P., Pašteka, R., Pohánka, V., Papčo, J., Milo, P., 2014. Detecting Shallow Medieval Features in the Church of St. George, Slovakia. Near Surface Geoscience 2014-20thEuropean Meeting of Environmental and Engineering Geophysics https://doi.org/10.3997/2214-4609.20141975.

Papadopoulos, T.D. and collaborators, 2003. Investigation of the deep structure of Central-west Attica with the contribution of geophysical soundings. OASP Applied research program, 90p., Athens (In Greek).

Papadopoulos, T.D., Goulty, N., Voulgaris, N.S., Alexopoulos, J.D., Fountoulis, I., Kambouris, P., Karastathis, V., Peirce, C., Chailas, S., Kassaras, J., Pirli, M., 2007. Tectonic structure of Central-Western Attica (Greece) based on geophysical investigations-preliminary results. Bull. Geol. Soc. Greece 40 (3), 1207–1218.

Papanikolaou, D. and collaborators, 2002. Geological – Geotechnical study of Athens basin. OASP Applied research program, 152p, Athens (*in Greek*).

Papanikolaou, D., Papanikolaou, I., 2007. Geological, geomorphological and tectonic structure of NE Attica and seismic hazard implications for the northern edge of the Athens plain. Bull. Geol. Soc. Greece 40, 425–438.

Radogna, P.V., Olivier, R., Logean, P., 2003. Micro-gravity survey in urban environment: modelling, evaluation and correction of buildings influence. 9th EAGE/EEGS Meeting https://doi.org/10.3997/2214-4609.201414579.

Stoulos, S., Manolopoulou, M., Papastefanou, C., 2003. Assessment of natural radiation exposure and radon exhalation from building materials in Greece. J. Environ. Radioact. 69 (3), 225–240. https://doi.org/10.1016/S0265-931X(03)00081-X.

Szeto, A., 2006. How Well Can One Determine the Density of a Box-like Building Using Gravity Measurements? 19th EEGS Symposium on the Application of Geophysics to Engineering and Environmental Problems

Wang, G., Zhu, Y., Zhang, S., Yan, C., Song, Y., Ma, Z., Hong, D., Chen, T., 2012. 3D geological modeling based on gravitational and magnetic data inversion in the Luanchuan ore region, Henan Province, China. J. Appl. Geophys. 80, 1–11 Micro-gravity survey in urban environment: modelling, evaluation and correction of buildings influence. https://doi.org/10.1016/j.jappgeo.2012.01.006.

Yan, Y., Gao, F., Deng, S., Su, N., 2017. A Hierarchical Building Segmentation in Digital Surface Models for 3D Reconstruction. Sensors 17 (2), 222. https://doi.org/10.3390/s17020222.

Yu, D., 2014. The Influence of buildings on Urban Gravity surveys. J. Environ. Eng. Geophys. 19 (3), 157–164. https://doi.org/10.2113/JEEG19.3.157.

Zheng, T., Chen, L., Zhao, L., Xu, W., Zhu, R., 2006. Crust–mantle structure difference across the gravity gradient zone in North China Craton: seismic image of the thinned continental crust. Phys. Earth Planet. Inter. 159 (1), 43–58. https://doi.org/10.1016/j.pepi.2006.05.004.